Molecular Therapy
Methods & Clinical Development
Original Article

UTX/KDM6A deletion promotes the recovery of spinal cord injury by epigenetically triggering intrinsic neural regeneration

Zhu Guo,[1,4,5,6] Chengjun Li,[1,2,6] Yong Cao,[1,2] Tian Qin,[1,2] Liyuan Jiang,[1,2] Yan Xu,[2,3] Miao Li,[1,2] Zixiang Luo,[1,2] Jianzhong Hu,[1,2] and Hongbin Lu[2,3]

[1]Department of Spine Surgery and Orthopedics, Xiangya Hospital, Central South University, Changsha 410008, China; [2]Key Laboratory of Organ Injury, Aging and Regenerative Medicine of Hunan Province, Changsha 410008, China; [3]Department of Sports Medicine, Research Centre of Sports Medicine, Xiangya Hospital, Central South University, Changsha 410008, China; [4]Spine Surgery Department of the Affiliated Hospital of Qingdao University, Qingdao 266000, China; [5]Traumatic Orthopedic Institute of Shandong Province, Affiliated Hospital of Qingdao University, Qingdao 266000, China

Interrupted axons that fail to regenerate mainly cause poor recovery after spinal cord injury (SCI). How neurons epigenetically respond to injury determines the intrinsic growth ability of axons. However, the mechanism underlying epigenetic regulation of axonal regeneration post-SCI remains largely unknown. In this study, we elucidated the role of the epigenetic regulatory network involving ubiquitously transcribed tetratricopeptide repeat on chromosome X (UTX)/microRNA-24 (miR-24)/NeuroD1 in axonal regeneration and functional recovery in mice following SCI. Our results showed that UTX was significantly increased post-SCI and repressed axonal regeneration *in vitro*. However, downregulation of UTX remarkably promoted axonal regeneration. Furthermore, miR-24 was increased post-SCI and positively regulated by UTX. miR-24 also inhibited axonal regeneration. Chromatin immunoprecipitation (ChIP) indicated that UTX binds to the miR-24 promoter and regulates miR-24 expression. Genome sequencing and bioinformatics analysis suggested that NeuroD1 is a potential downstream target of UTX/miR-24. A dual-luciferase reporter assay indicated that miR-24 binds to NeuroD1; moreover, it represses axonal regeneration by negatively regulating the expression of NeuroD1 via modulation of microtubule stability. UTX deletion *in vivo* prominently promoted axonal regeneration and improved functional recovery post-SCI, and silencing NeuroD1 restored UTX function. Our findings indicate that UTX could be a potential target in SCI.

INTRODUCTION

Spinal cord injury (SCI) is a devastating central nervous system (CNS) disease that can cause permanent sensory and motor dysfunction.[1] The annual incidence of traumatic SCI is approximately 11.5–54 per 1 million people worldwide.[2–4] SCI causes great physical and psychological trauma to individuals, and recovery after SCI remains extremely difficult and is a great global challenge.[5–7]

Acute SCI usually leads to a loss of sensory and motor function below the injury plane, which is attributed to immediate axonal interruption caused by the injury.[8] The recovery of spinal function is unsatisfactory in most cases because regeneration of interrupted axons is very limited.[9,10] The inherent lack of intrinsic growth potential of the mature CNS neurons is one of the main factors that limits axonal regeneration.[11] Increasing evidence has indicated that epigenetic regulation plays a significant role in modulating neurogenesis, neuroplasticity, and CNS regeneration.[12–14]

Compared to the peripheral nervous system (PNS), the CNS has a limited ability to regenerate since the epigenetic responses to axonal injury are quite different, which indicates that epigenetic regulation may be a major factor affecting axonal regeneration.[13,15–17] However, effective epigenetic targets that work in parallel with the neuron intrinsic regeneration program remain to be identified. Epigenetic modifications can regulate gene expression without altering gene sequences, thereby causing phenotypic changes.[18] Histone methylation is one form of histone modification, and the histone methylation status affects the advanced chromatin structure, which is closely related to gene expression.[19] Ubiquitously transcribed tetratricopeptide repeat on chromosome X (UTX), also known as KDM6A, removes the inhibitory trimethylation of histone 3 lysine 27 (H3K27me3) and transforms genes to an active state.[20] Knocking out UTX in neural progenitor cells can promote proliferation while inhibiting differentiation by affecting the PTEN/Akt/mTOR signaling pathway.[21] A loss of

Received 28 June 2020; accepted 2 December 2020;
https://doi.org/10.1016/j.omtm.2020.12.004.

[6]These authors contributed equally

Correspondence: Jianzhong Hu, Department of Spine Surgery and Orthopedics, Xiangya Hospital, Central South University, Changsha 410008, China.
E-mail: jianzhonghu@hotmail.com
Correspondence: Hongbin Lu, Department of Sports Medicine, Research Centre of Sports Medicine, Xiangya Hospital, Central South University, Changsha 410008, China.
E-mail: hongbinlu@hotmail.com
Correspondence: Yong Cao, Department of Spine Surgery and Orthopedics, Xiangya Hospital, Central South University, Changsha 410008, China.
E-mail: caoyong1912@163.com

UTX can have a significant effect on the expression of 5-HT receptors, thus leading to neuronal morphological abnormalities.[22,23] Although UTX plays an indispensable role in nervous system development, the function of UTX in CNS injury has rarely been reported. We previously reported that knocking out UTX in vascular endothelial cells can epigenetically promote vascular regeneration post-SCI.[24] However, whether UTX functions as a regulator of axonal regeneration after SCI has not been reported.

MicroRNAs (miRNAs) are highly conserved small noncoding RNAs (less than 22 nucleotides in length) that regulate posttranscriptional gene expression.[25] miRNAs have been reported to play an important role in repair after SCI.[26–28] In our previous study, microarray analysis identified microRNA-24 (miR-24) as a significantly differentially expressed miRNA after SCI.[29] Therefore, miR-24 is likely to be associated with axonal regeneration.

Neurogenic differentiation 1 (NeuroD1) is a member of the basic helix-loop-helix (bHLH) transcription factor family and plays an essential role during neurogenesis and neuronal differentiation, survival, and maturation in the CNS.[30] Recent studies have proven that NeuroD1 can facilitate axonal growth and promote functional recovery after sciatic nerve injury.[31] However, the function of NeuroD1 in SCI remains elusive.

In this study, we report the mechanism of an epigenetic regulatory network involving UTX/miR-24/NeuroD1, which regulates axonal regeneration and recovery of spinal function post-SCI.

RESULTS

Expression of UTX increases in mouse spinal cord neurons post-SCI

To verify the potential participation of UTX in epigenetic regulation post-SCI, we detected the expression of UTX in the lesion in a mouse hemisection SCI model. Quantitative real-time PCR (qRT-PCR) indicated that UTX expression was significantly increased 3 days post-SCI and remained at a high level at 7 and 14 days post-SCI (Figure 1B). Immunofluorescence staining of the spinal cord lesion demonstrated that UTX expression was primarily increased in the nuclei of $NeuN^+$ neurons (Figures 1A and 1C). However, the increase in UTX expression in $Neun^-$ cells was relatively low (Figure 1D). The marked square in Figure 1G shows the area in the representative images. The activation of UTX expression implies that it is potentially involved in the epigenetic response post-SCI.

UTX is an intrinsic inhibitor of axonal regrowth *in vitro*

Since we know that UTX is significantly increased in response to SCI, we determined whether it affects axonal regrowth. We regulated the expression of UTX with a UTX-expressing lentivirus (LV) and a UTX short hairpin RNA (shRNA)-expressing lentivirus and verified the overexpression and knockdown efficiencies by qRT-PCR (Figure S1). Immunofluorescence staining of TUJ1 was performed to label neuronal axons. UTX significantly inhibited cortical neuron axonal regrowth, while UTX downregulation significantly promoted axonal regrowth (Figures 2A and 2D), suggesting that UTX is an intrinsic inhibitor of axonal regrowth.

miR-24 is upregulated post-SCI and inhibits axon regeneration by impairing microtubule stability

In our previous study, we reported that miR-24 is one of the most differentially expressed miRNAs post-SCI.[29] In this study, we performed *in situ* hybridization of miR-24 to verify the change in its expression. The results indicated that miR-24 was significantly increased in $NeuN^+$ neurons at the lesion site 14 days post-SCI (Figures 1E and 1F). In addition, we found that miR-24 upregulation impaired microtubule stability and inhibited cortical neuron axon regeneration while miR-24 downregulation improved microtubule stability and significantly promoted axonal regeneration (Figures 2B, 2C, 2E, and 2F).

UTX and miR-24 form an epigenetic complex that inhibits axonal regeneration

Since UTX is increased post-SCI and can epigenetically demethylate H3K27me3 and activate target genes, we wondered whether UTX induces miR-24 expression. Thus, we detected the ability of UTX to regulate miR-24. We found that knocking down UTX increased the methylation of H3K27me3 (Figures 3A and 3B) and repressed the expression of miR-24 (Figure S2B), while UTX upregulation significantly increased the expression of miR-24 (Figure S2A). In addition, we carried out chromatin immunoprecipitation (ChIP)-qPCR to detect the potential binding between UTX and the miR-24 promoter. The results provided solid evidence that UTX directly binds to the promoter of miR-24 (Figures 3C–3E). All the results indicate that UTX positively regulates miR-24 through demethylation of the miR-24 promoter.

In addition, we further explored whether UTX-induced inhibition of axonal regeneration is dependent on microtubule destabilization by miR-24. We carried out a miR-24 loss-of-function assay and found that axonal deacetylation and axonal suppression of UTX were abolished when miR-24 was silenced (Figures 3F–3I). Taken together, the binding results and the loss-of-function assay results suggest that UTX and miR-24 form an epigenetic complex and inhibit axonal regeneration by destabilizing microtubules and that the inhibition of axonal regeneration is miR-24 dependent.

NeuroD1 is a downstream target of UTX/miR-24

To determine the mechanism by which UTX/miR-24 regulates axonal regeneration, we downregulated UTX in cortical neurons and screened differentially expressed mRNAs using whole-genome sequencing (Figure S3). There were 1,421 upregulated genes and 715 downregulated genes (Figure 4A). We then picked out 52 UTX-regulated genes related to neuron development (Figure 4B). We further predicted the downstream target of miR-24 by using miRNA target prediction tools (http://www.targetscan.org; http://www.mirdb.org/). A Venn diagram showed that NeuroD1 is a common target of UTX and miR-24 (Figure 4C). The 3′ UTR of NeuroD1

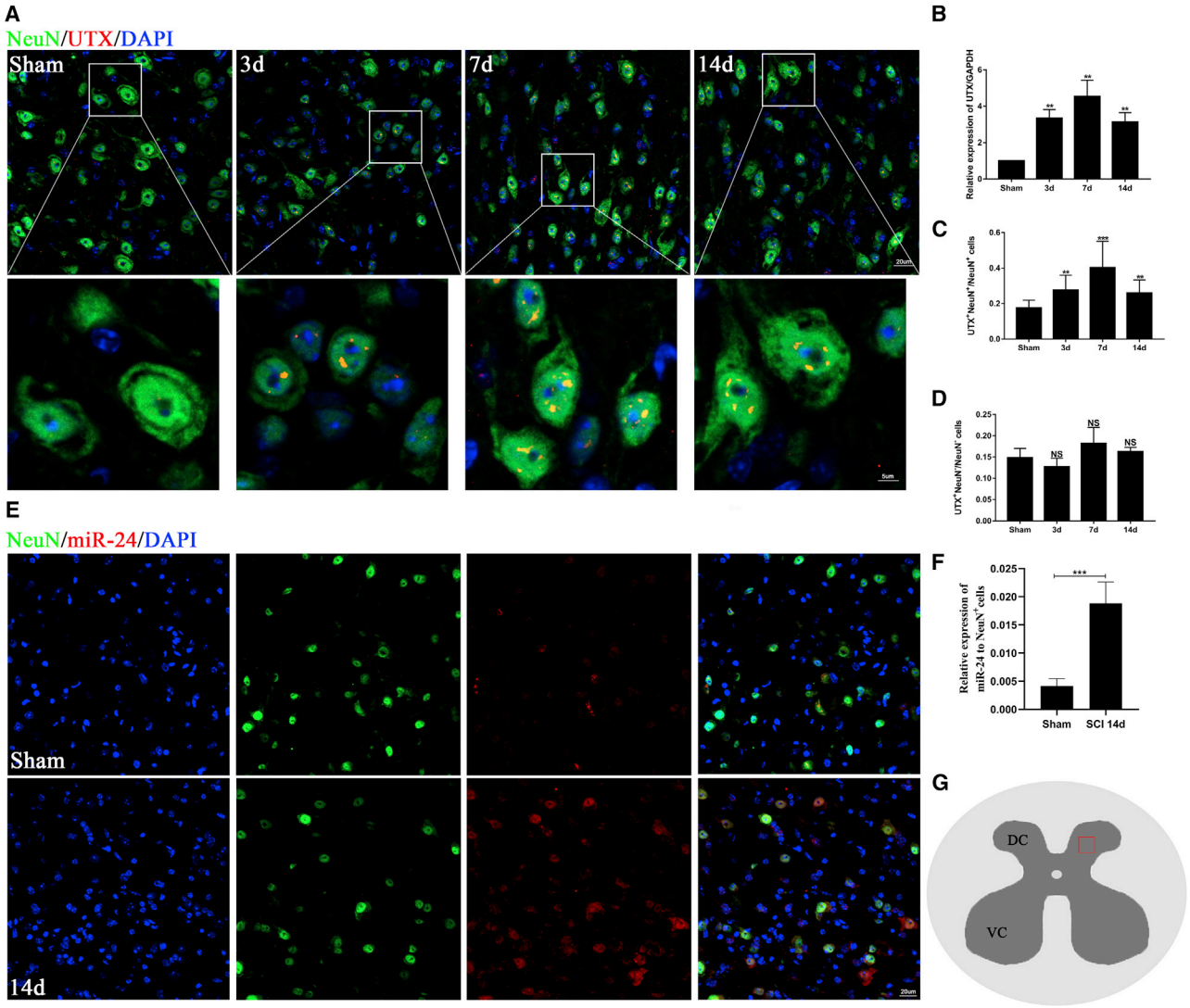

Figure 1. Expression of UTX in neurons was increased after spinal cord injury

(A) Representative images of double staining with NeuN (green) and UTX (red) at different time points. Nuclei were stained with DAPI (blue). The scale bars in the upper panels represent 20 μm, while those in the lower panels represent 5 μm (n = 4). (B) qRT-PCR analysis of UTX and GAPDH expression at different time points (n = 3). (C) Quantitative ratio of UTX + $NeuN^+$ cells to $NeuN^+$ cells in (A). (D) Quantitative ratio of UTX + $NeuN^-$ cells to $NeuN^-$ cells in (A). (E) *In situ* hybridization of miR-24 (red) and fluorescence staining of NeuN (green) at the lesion site 14 days post-SCI (n = 4). (F) Quantification of miR-24-positive staining in (E). (G) Marked square showing the area in the representative images. Data are presented as the mean ± SD. **p < 0.01; ***p < 0.001; ns, not significant.

contains a complementary sequence for miR-24-3p (Figure 4E). We then performed a dual-luciferase reporter assay to verify the direct relationship between miR-24 and NeuroD1. The results showed that agomir-24 (a miR-24 mimic) reduced luciferase activity in cells carrying wild-type NeuroD1, while no change in luciferase activity was observed in cells carrying mutant NeuroD1 and those transfected with the miRNA control virus (Figure 4D), which indicates that miR-24 can directly bind to the 3′ UTR of NeuroD1. In addition, we further confirmed the ability of UTX/miR-24 to epigenetically regulate NeuroD1. The qRT-PCR and western blot results showed that downregulating UTX or miR-24 significantly promoted NeuroD1 expression, while miR-24 upregulation reduced the expression of NeuroD1 (Figures 4F–4K). These results suggest that NeuroD1 is a downstream target of UTX/miR-24.

miR-24 can regulate microtubule stabilization and axonal growth by targeting NeuroD1

To further investigate the axon-promoting function of UTX/miR-24 involving NeuroD1 regulation, we constructed a NeuroD1-overexpressing lentivirus. The western blot results showed that NeuroD1 upregulation by LV-NeuroD1 increased the expression of acetylated microtubules (Figures 5A and 5B), and immunofluorescence also

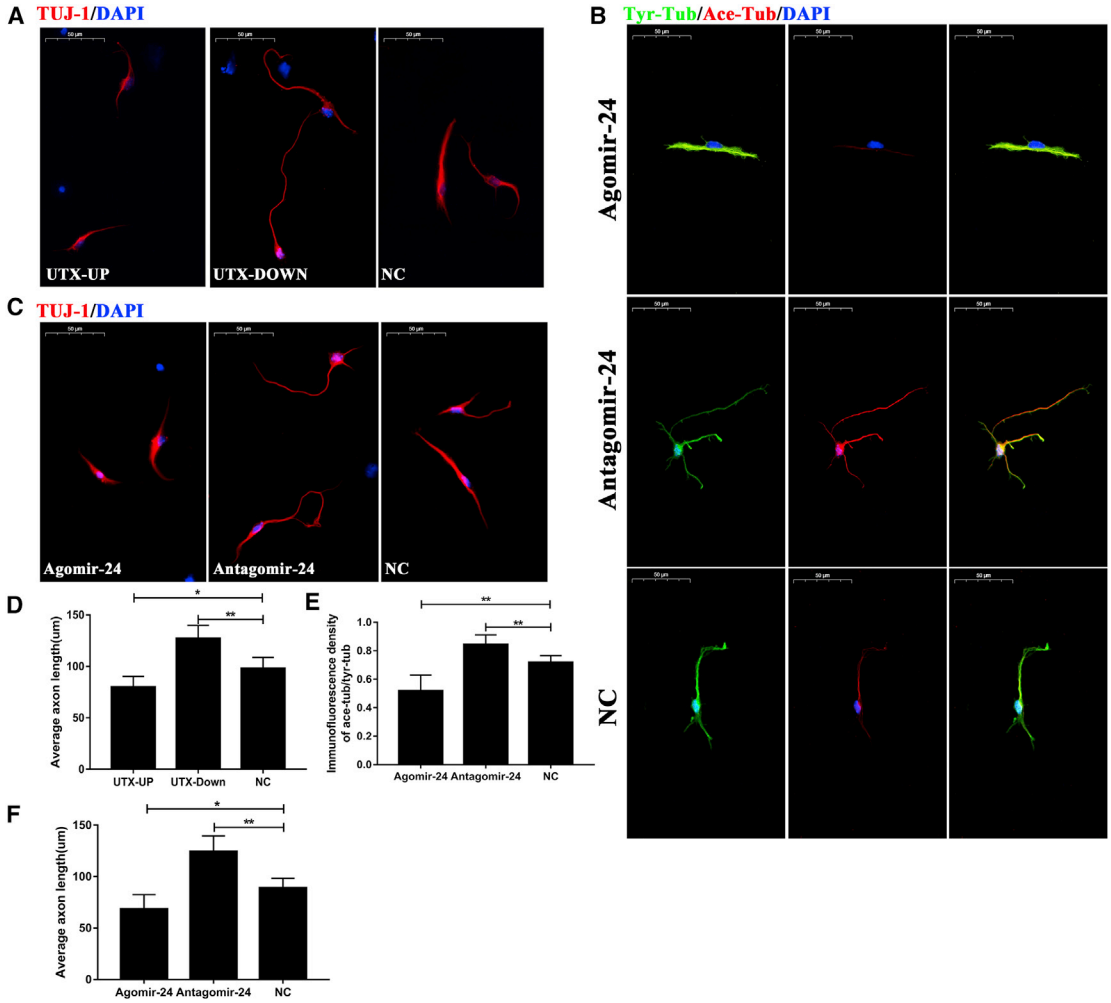

Figure 2. UTX and miR-24 are intrinsic inhibitors of axon regrowth

(A) Representative immunofluorescence images of TUJ1 (red) in the UTX-up group, UTX-down group, and control group (n = 5). (B) Representative images of immunofluorescence staining of tyrosinated tubulin (green) and acetylated tubulin (red) in the agomir-24 group, antagomir-24 group, and control group (n = 5). (C) Representative immunofluorescence images of TUJ1 (red) in the agomir-24 group, antagomir-24 group, and control group (n = 5). (D) Quantification of the average axon length in (A). (E) Quantitative ratio of acetylated tubulin to tyrosinated tubulin in (B). (F) Quantification of the average axon length in (C). Data are presented as mean ± SD. Scale bar, 10 μm; *$p < 0.05$; **$p < 0.01$.

showed that NeuroD1 upregulation promoted axonal growth (Figures 5C and 5D).

To further investigate whether miR-24 regulates microtubule stabilization and axonal growth by targeting NeuroD1, we simultaneously downregulated miR-24 and NeuroD1 in neurons. The immunofluorescence staining results indicated that NeuroD1 downregulation abolished the ability of miR-24 silencing to promote microtubule acetylation and axonal growth (Figures 5E–5H).

UTX deletion in neurons within the lesion improves recovery of spinal function post-SCI in a NeuroD1-dependent manner

To explore whether UTX deletion improves spinal function recovery after acute SCI, we knocked out UTX in the corticospinal tract (CST) by injecting adeno-associated virus(AAV)-cre-EGFP into the hindlimb sensorimotor area of the cerebral cortex 2 weeks before SCI. The Basso mouse scale (BMS) was applied to assess motor function recovery. Better recovery was observed in UTX knockout mice as early as 3 weeks and until 8 weeks postinjury (Figure 6A). Sensory function evaluation was performed at the same time. Two weeks after injury, tactile sensory function began to recover gradually. Recovery of the tactile sensory function in UTX knockout mice was significantly better than that in the control group from the second week until the eighth week (Figure 6B). Mice with UTX knockdown in the CST showed better thermal sensory recovery from 2 weeks postinjury to the terminal time point (Figure 6C). From 8 to 10 weeks, the recovery of motor and sensory function reached a plateau. We performed neuroelectrophysiology to evaluate axonal conductivity 8 weeks

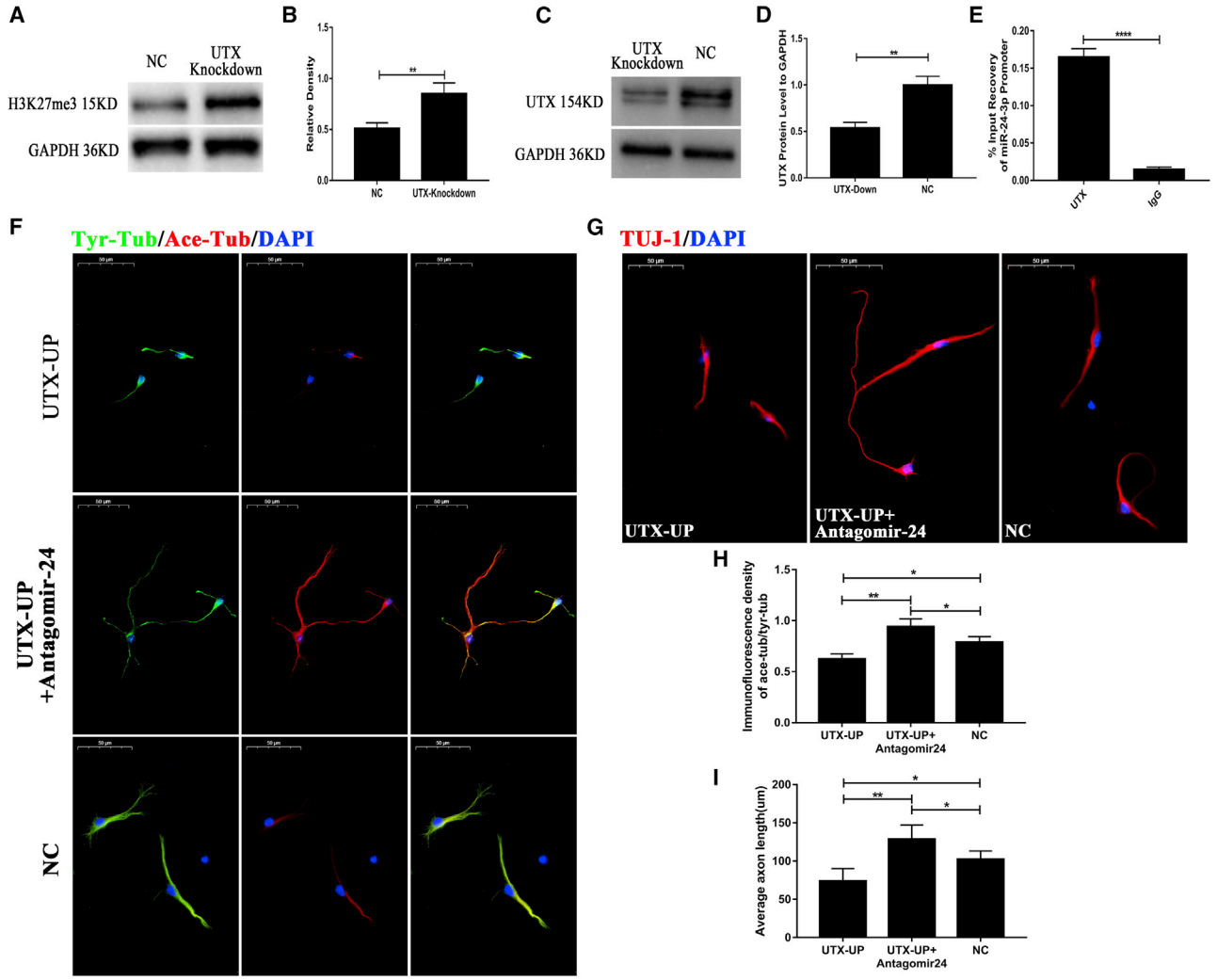

Figure 3. UTX and miR-24 form an epigenetic complex that inhibits axon regrowth

(A) Western blot analysis of H3K27me3 and GAPDH in the UTX knockdown group and control group (n = 3). (B) Quantification of (A). (C) Western blot analysis of UTX and GAPDH in the immunoprecipitation products of the UTX knockdown group and control group (n = 3). (D) Quantification of (C). (E) Expression levels of the miR-24 promoter and GAPDH promoter in the immunoprecipitation products of the UTX pull-down group and IgG pull-down group as determined by qPCR (n = 3). (F) Representative images of immunofluorescence staining of tyrosinated tubulin (green) and acetylated tubulin (red) in the UTX-up group, UTX-up+antagomir-24 group, and control group (n = 3). (G) Representative images of TUJ1 (red) in the UTX-up group, UTX-up+antagomir-24 group, and control group (n = 5). (H) Quantitative ratio of acetylated tubulin to tyrosinated tubulin in (F). (I) Quantification of the average axon length in (G). Data are presented as the mean ± SD. Scale bar, 10 μm; *p < 0.05; **p < 0.01; ****p < 0.0001.

postinjury. A neuroelectrophysiological analysis of motor-evoked potentials (MEPs) indicated that UTX knockout mice exhibited a larger maximum amplitude and shorter latent period than control mice, indicating that UTX deletion promoted nerve conduction (Figures 6D–6F). To determine whether the improvements were dependent on NeuroD1, we performed a NeuroD1 loss-of-function assay. NeuroD1 shRNA abolished the functional improvement induced by UTX deletion, which indicated that UTX deletion-mediated axonal regeneration is dependent on NeuroD1. To determine whether the recovery of function was caused by the growth of regenerative nerves in the damaged area, at 10 weeks + 1 day after the first hemisection, we performed a second hemisection in the same location as the first. We found that spinal function was lost, suggesting that the previous improvement in sensorimotor activity was due to axon regeneration (Figures 6A–6D).

UTX deletion facilitates axonal regeneration by stabilizing axonal microtubules *in vivo*

Western blot analysis and immunofluorescence staining were performed to verify the UTX knockdown efficiency *in vivo*. Compared with that in the control mice (SCI only), the protein expression of UTX in UTX knockdown mice was significantly decreased on the

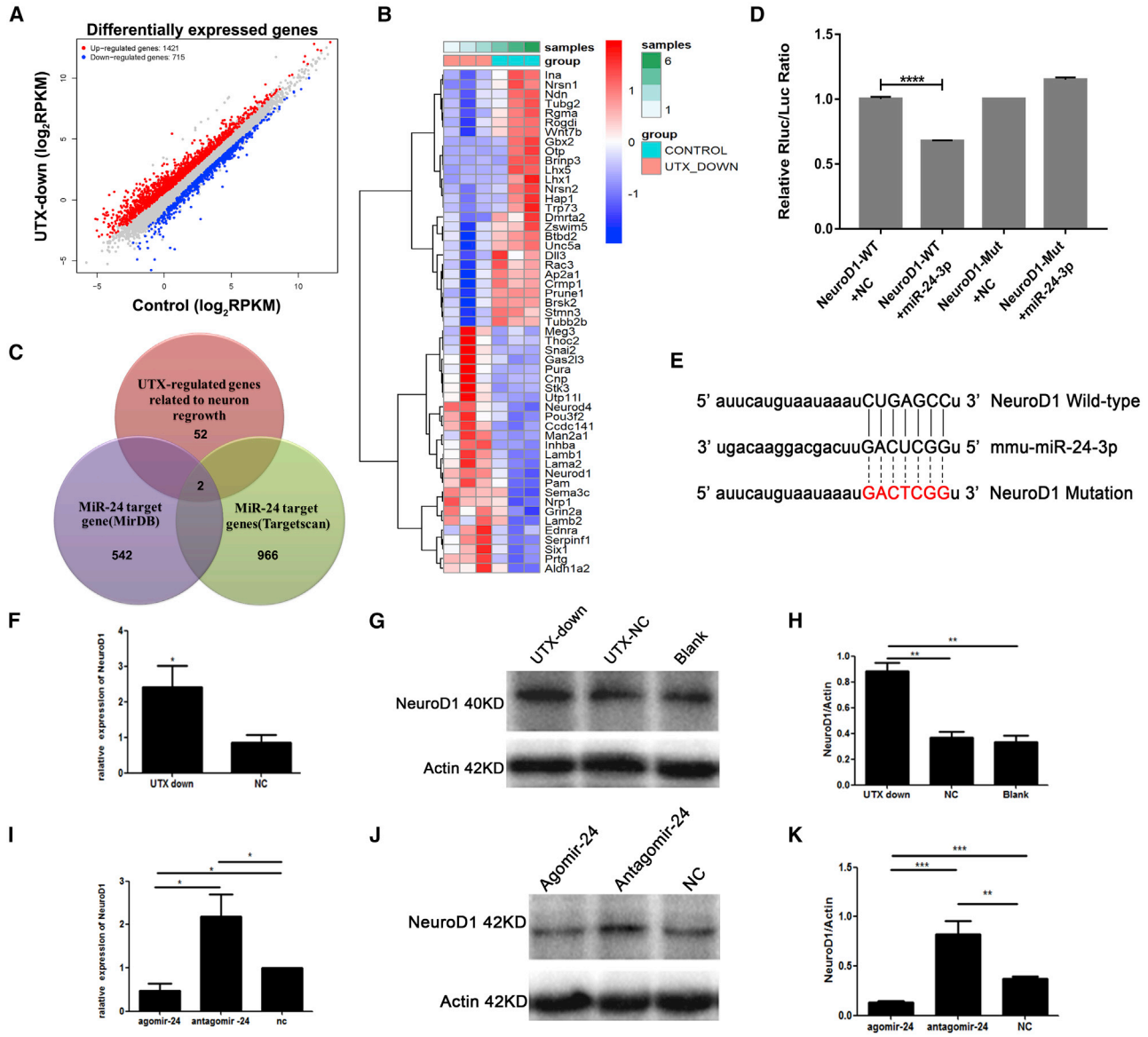

Figure 4. NeuroD1 is a downstream target of UTX/miR-24

(A) Volcano plot of the upregulated genes and downregulated genes (fold change > 1.5; $p < 0.05$; n = 3). (B) Cluster analysis of the neurological system-related genes. (C) UTX-regulated genes related to neuron regrowth and the prediction of miR-24-targeted mRNAs by TargetScan and miRDB. (D) Relative luciferase activities in the human renal epithelial cells (293T cells) of the NeuroD1-wild-type (WT) + negative control group, NeuroD1-WT + miR-24-3p group, NeuroD1-mutant (mut) + negative control group, and NeuroD1-mut + miR-24-3p group (n = 3). (E) The complementary sequences between miR-24-3p and the 3′ UTR of NeuroD1. (F) Expression levels of NeuroD1 and GAPDH in the UTX-down group and control group as determined by qRT-PCR (n = 3). (G and H) Western blot analysis (G) and quantification (H) of NeuroD1 and actin in neurons of the UTX down group, negative control group, and blank group (n = 3). (I) Expression levels of NeuroD1 and GAPDH in the agomir-24 group, antagomir-24 group, and control group as determined by qRT-PCR (n = 3). (J and K) Western blot analysis (J) and quantification (K) of NeuroD1 and actin in the neurons of the agomir-24 group, antagomir-24 group, and control group (n = 3). Data are presented as the mean ± SD; *$p < 0.05$; **$p < 0.01$; ***$p < 0.001$; ****$p < 0.0001$.

third day after injury (Figure S4). Costaining for UTX and NeuN further validated the UTX knockout efficiency (Figure S5). Immunofluorescence staining for NeuN and acetylated tubulin was performed. As shown in the fluorescence images (Figure 7A), acetylated tubulin (Ace-tub) was obviously increased in the UTX knockdown mice compared with the control mice 8 weeks postinjury, which was further confirmed by western blot analysis (Figures 7B and 7C). Western blot analysis (Figures 7B and 7C) and immunofluorescence staining (Figure 7A) also indicated that UTX deletion-mediated acetylated tubulin expression was dependent on NeuroD1. Taken

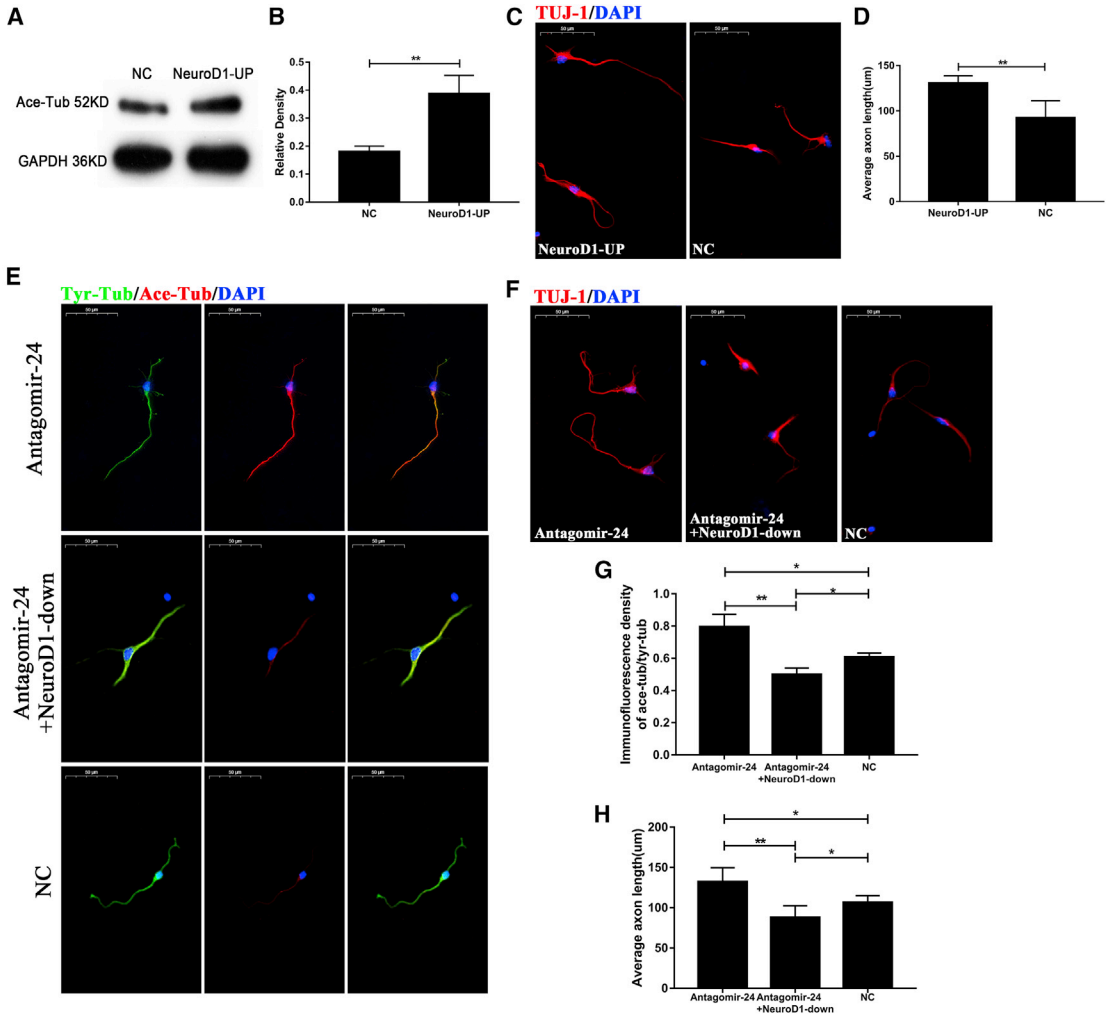

Figure 5. miR-24 regulates microtubule stabilization and axon growth by directly targeting NeuroD1

(A) Western blot analysis of acetylated tubulin and GAPDH in the NeuroD1-up group and control group (n = 3). (B) Quantification of (A). (C) Representative images of TUJ1 (red) in the NeuroD1-up group and control group (n = 5). (D) Quantification of the average axon length in (C). (E) Representative images of tyrosinated tubulin (green) and acetylated tubulin (red) in the antagomir-24 group, antagomir-24+NeuroD1-down group, and control group (n = 3). (F) Representative images of TUJ1 (red) in the antagomir-24 group, antagomir-24+NeuroD1-down group, and control group (n = 5). (G) Quantitative ratio of acetylated tubulin to tyrosinated tubulin in (E). (H) Quantification of the average axon length in (F). Data are presented as the mean ± SD. Scale bar, 10 μm; *p < 0.05; **p < 0.01.

together, these findings demonstrate that UTX has a negative effect on the acetylation levels of microtubules by regulating NeuroD1. To verify the axon-promoting effect of UTX deletion after SCI, longitudinal sections of the spinal cord were stained with an anti-TUJ1 antibody. The intensity of TUJ1 staining in the injury area was statistically higher (Figures 7D and 7E) in the UTX knockout mice than the control mice. We obtained frozen sections from below the injury site (Figure S6B) and labeled serotonergic neurons with a 5-HT antibody. We found that the 5-HT-positive area was significantly larger in UTX knockout than control mice (Figures S6A–S6C). To investigate the effect of UTX deletion on the regeneration of the CST, we performed biotin dextran amine (BDA) antegrade tracing (Figure 7F). In the UTX knockout mice, a large number of axons regenerated and crossed the lesion site, whereas in the control group, almost no axons regenerated and crossed the injury site. In addition, NeuroD1 shRNA abolished the axon-promoting effects of UTX deletion, which indicated that axonal regeneration mediated by UTX deletion is NeuroD1 dependent. Therefore, these results demonstrate that UTX deletion *in vivo* can promote axonal regeneration by enhancing microtubule stability.

DISCUSSION

Acute SCI often leads to permanent loss of sensory and motor function. Poor functional recovery following CNS injury is mainly attributed to the failure of interrupted axons to regenerate and form new functional connections.[3,4] The mature CNS has a more complex

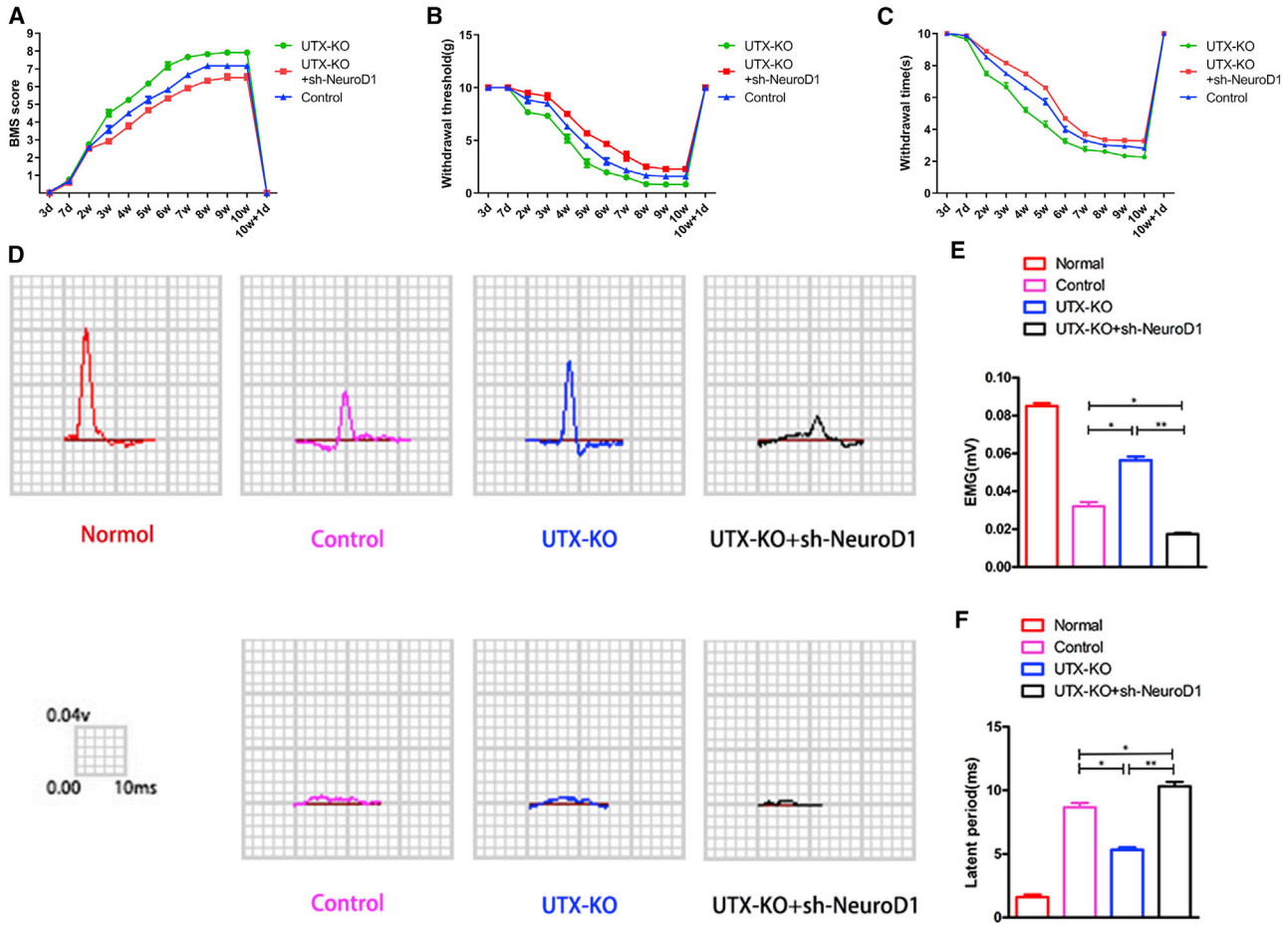

Figure 6. Knockdown of UTX in the cortical spinal tract facilitated neurological function recovery after SCI by targeting NeuroD1

(A) Functional analysis of the UTX-knockout (KO) group, UTX-KO + NeuroD1-down group, and control group postinjury using the BMS scoring system (n = 12). (B) Tactile sensory function of the UTX-KO group, UTX-KO + NeuroD1-down group, and control group over time after spinal cord injury as determined by the Von Frey filament test (n = 12). (C) Thermal sensory function of the UTX-KO group, UTX-KO + NeuroD1-down group, and control group over time after spinal cord injury (n = 12). (D) Neuro-electrophysiological analysis of the normal group, control group, UTX-KO group, and UTX-KO + NeuroD1-down group at 8 weeks and 8 weeks + 1 day postinjury (n = 3). (E) Quantification of the amplitude of MEP in (D). (F) Quantification of the latent period of MEP in (D). Data are presented as the mean ± SD; *p < 0.05; **p < 0.01.

structure and superior function than the developing CNS or PNS; however, the evolutionary price of these differences is a reduced ability to regenerate after axonal injury.[14]

In the mammalian CNS, the axonal growth gene program is believed to shut down once neurons mature, while inhibitory genes are upregulated and intrinsic axonal growth potential is suppressed.[32] The axonal regeneration program remains inactive even when axons are injured. Phenotypic transition is the result of progressive changes in the chromatin profile that ensure the stable expression of underlying genes.[33] However, the developmental chromatin status becomes an epigenetic barrier to mature CNS neuron axonal regeneration. Thus, it is crucial to remove the epigenetic restriction of injured neurons to reboot the regenerative transcriptional program and allow regrowth.

Histone methylation is one of the classical epigenetic mechanisms that regulates gene expression. UTX is an important histone demethylase that is located on the X chromosome and mediates the demethylation process of H3K27me3/me2 to activate gene expression. UTX alters the state of H3K27, which contributes to embryonic development, stem cell differentiation, and CNS oncogenesis.[34,35] However, knowledge of how UTX modulates CNS repair is lacking. We previously demonstrated that UTX is a key epigenetic factor that inhibits vascular regeneration after SCI. In the present study, we found that UTX deletion promotes axonal regeneration and facilitates functional recovery after SCI.

Our results indicated that UTX expression increased in response to SCI and that UTX directly bound to the miR-24 promoter and removed the inhibitory methyl group from H3K27me3, which caused

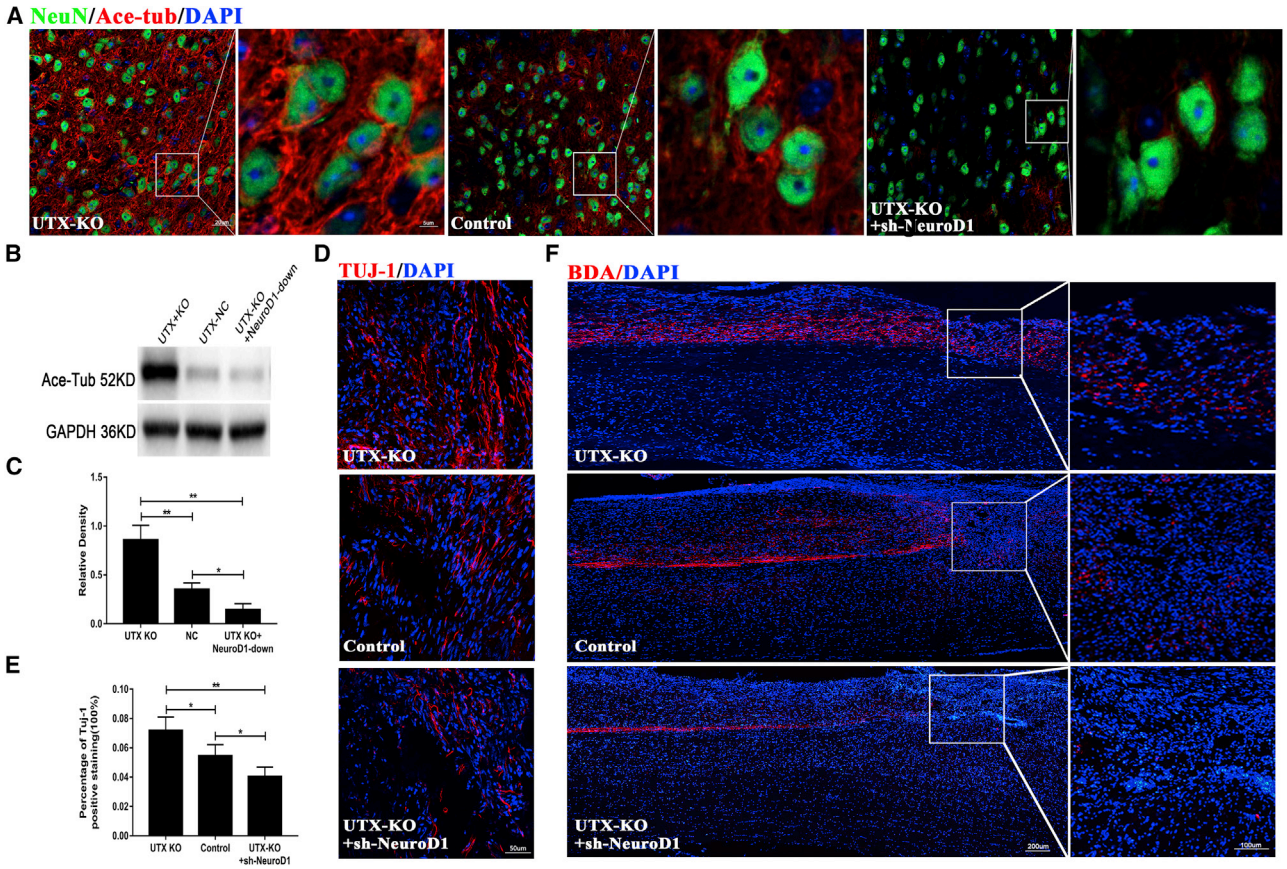

Figure 7. UTX deletion improves axon regeneration by stabilizing axonal microtubules *in vivo*

(A) Representative images of NeuN (green) and acetylated tubulin (red) in the UTX-KO group, control group, and UTX-KO + NeuroD1-down group (n = 5). Scale bars, 20 μm and 5 μm. (B) Western blot analysis of acetylated tubulin and GAPDH in the UTX-KO group, control group, and UTX-KO + NeuroD1-down group (n = 3). (C) Quantification of (B). (D) Immunofluorescence images of TUJ1 for the determination of axon density in the UTX-KO group, control group, and UTX-KO + NeuroD1-down group (n = 4). Scale bar, 50 μm. (E) Quantification of TUJ1-positive staining in (D). (F) Spinal sections immunostained for BDA (n = 3). Scale bars, 200 μm for the left panels and 100 μm for the right panels. Nuclei were immunostained with DAPI. Data are presented as the mean ± SD; *p < 0.05; **p < 0.01.

epigenetic activation of miR-24 expression. Interestingly, UTX acts as an epigenetic regulator and regulates miRNAs, which are also epigenetic factors. Our results proved that UTX positively regulates and forms an epigenetic complex with miR-24. In addition, we demonstrated that the inhibitory effect of UTX/miR-24 on axon regeneration is dependent on the epigenetic repression of NeuroD1 by miR-24.

The expression of regeneration-associated genes (RAGs) is affected by injury, and these genes are functionally required for neural regeneration.[17,36] The absence of key responses by RAGs in CNS neurons is the main cause of axonal regeneration failure even when extrinsic inhibitors are removed or replaced with a favorable environment.[11,37] NeuroD1 is a bHLH transcription factor that plays a crucial role in neuronal genesis and differentiation, and it possesses the ability to elicit the neuronal development program, suggesting that upregulation of NeuroD1 in injured neurons may transform them into a less-mature state.[38] Our results suggest that NeuroD1 is a potential RAG that can promote axonal regeneration by enhancing microtubule stability. In addition, we found that NeuroD1 is a direct target of miR-24 and is epigenetically suppressed by UTX/miR-24. Our results suggest that SCI triggers the upregulation of UTX/miR-24, which epigenetically represses NeuroD1 and consequently results in inhibition of the intrinsic growth potential that makes neurons unable to enter the regenerative program. Removing the repressive effects of UTX/miR-24 can promote axonal regeneration and improve functional recovery post-SCI. However, activation of NeuroD1 is indispensable for this epigenetic regulation of the axonal regeneration mechanism.

It has been documented that microtubule stabilization is closely related to axonal growth.[39–42] After CNS injury, disrupted axons form numerous retraction bulbs with disorganized microtubules.[43] Antitumor drugs, such as paclitaxel and epothilone B, which act as microtubule-stabilizing agents, have been reported to promote axonal regeneration and reduce scar formation after SCI.[44,45] Although we

observed that overexpression of NeuroD1 enhanced microtubule stabilization, we did not further investigate how NeuroD1 regulates microtubule stabilization in neurons. However, microtubule stabilization depends largely on the level of acetylated tubulin, and the ratio of acetylated tubulin/tyrosinated tubulin can be used to reflect the microtubule stability of axons. In our study, we mainly focused on the regulatory effect of the epigenetic network on innate regrowth potential and resulting axonal regeneration and functional recovery. The mechanism by which NeuroD1 affects microtubule stability remains to be further studied.

In conclusion, our study demonstrated that UTX/miR-24 may form an epigenetic complex and suppress the expression of NeuroD1, which limits the intrinsic regrowth potential of neurons. UTX deletion contributes to removing this barrier and activating NeuroD1, which triggers intrinsic neural regeneration and causes neurons to enter a premature state that favors regeneration. All the results suggest that UTX may be a promising therapeutic target in SCI.

MATERIALS AND METHODS

Animals

Adult female UTX$^{flox/flox}$ mice (stock no. 021926) weighing 18–22 g were purchased from the Jackson Laboratory. To knock out UTX in the CST, AAV-cre-EGFP was injected into the hindlimb sensorimotor area of the cerebral cortex 2 weeks before hemisection of the spinal cord: four injection sites, from bregma, −0.5/−0.5/0.7 mm, −0.5/−1.0/0.7 mm, −1.0/−0.5/0.7 mm, and −1.0/−1.0/0.7 mm anteroposterior/mediolateral/dorsoventral (AP/ML/DV). All procedures were carried out with the approval of the Laboratory Animal Users Committee at Xiangya Hospital, Central South University, Changsha, China.

Cell culture and treatment

Primary cortical neurons were extracted from the cerebral cortices of fetal C57BL/6 mice. In brief, the cerebral cortex was gently removed and washed twice with PBS. Next, the dura mater was carefully removed, and the cortex was separated and placed in Dulbecco's modified Eagle's medium (DMEM; HyClone, USA). Then, the cerebral cortical tissue was gently pipetted with a Pasteur pipette for homogenization. After centrifugation at 1,000 rpm for 5 min, the supernatant was carefully removed. The cells were resuspended and cultured with neurobasal medium (Cyagen, USA) containing 2% B27, 1% glutamine, and 1% penicillin-streptomycin and then transfected with LV-Kdm6a (Shanghai Genechem, Shanghai, China) (for UTX overexpression) at an MOI of 1:20. LV-Kdm6a-shRNA (MOI = 1:20), agomir-24 (200 nmol/mL, Ribo, Guangzhou, China), antagomir-24 (200 nmol/mL), and LV-NeuroD1 (MOI = 1:30, Shanghai Genechem, Shanghai, China) were used following the manufacturer's protocols.

Lateral hemisection SCI model

Adult female UTX$^{flox/flox}$ mice were used to establish a hemisection SCI model. After anesthetization and fur removal, a dorsal medial incision was made, and a T10 laminectomy was performed to expose the spinal cord. The spinal cord was cut transversely from the posterior spinal artery to the right edge with a sharp scalpel. Then, we used a needle (3#/30G) to puncture the spinal cord dorsoventrally at the midline and pulled the needle to cut the right half of the spinal cord. sh-NeuroD1 or corresponding control virus (Shanghai Genechem, Shanghai, China) was intrathecally injected into the injured area immediately after SCI. Then, the muscle and skin were sutured in sequence. After skin disinfection, the mice were placed on a thermostat blanket until fully awake.

BDA tracing

Ten percent BDA (10,000 MV, Invitrogen) was used to anterogradely label CST axons as previously described.[46] In brief, 6 weeks after SCI, the mice were anesthetized and fixed on a stereotactic instrument (Stoelting, USA). Then, the skull was exposed, and a burr hole was drilled over the sensorimotor area. BDA was injected into the sensorimotor cortex at 6 sites (0.4 μL/site) at a rate of 0.05 μL/min using a microinjector (from bregma, −1.0/−0.1/0.6 mm, −1.0/−0.6/0.6 mm, −1.0/−1.1/0.6 mm, −1.4/−0.1/0.6 mm, −1.4/−0.6/0.6 mm, and −1.4/−1.1/0.6 mm AP/ML/DV). After each injection, the microinjection needle was kept in place for 2 min to allow for BDA infiltration.

Locomotor function

Locomotor function was evaluated at 3, 7, 14, 21, 28, 35, 42, 49, 56, 63, 70, and 71 days postinjury using the BMS,[47] which ranges from 0 to 9 points (0 indicates complete paralysis, and 9 indicates no hindlimb movement impairment). Two well-trained investigators simultaneously observed hindlimb movement without knowledge of the animal grouping. Final scores were obtained by averaging the values assigned by both observers.

Von Frey filament test

Tactile sensory function was evaluated by the Von Frey filament test as previously described.[48] In brief, the mice were placed on a test platform in a quiet, undisturbed environment and acclimated for 30 min. A monofilament (IITC, USA) was used to stimulate the plantar surface of the hindpaw of each mouse. Starting with the lowest-intensity filament, filaments of increasing intensity were applied to the paw until they buckled. The minimum force that produced a positive reaction, such as rapid paw withdrawal or sudden hindpaw licking, was recorded as the withdrawal threshold. The experiment was repeated 3 times with an interval of 10 min. The test was performed at 3, 7, 14, 21, 28, 35, 42, 49, 56, 63, 70, and 71 days postinjury.

Unilateral Hargreaves thermal test

The Hargreaves method was used to assess thermal hyperalgesia using a plantar test apparatus as previously described.[49] The platform was preheated, and the temperature was set to 33°C. The standby light intensity was set to 5%, and the working light intensity was 40%. The maximum irradiation time was set to 10 s. The mice were placed on a thermostatic test platform and acclimated for 30 min. The plantar surface of the hindpaw was stimulated by a thermal radioluminescence apparatus (IITC, USA). Irradiation was terminated when the mouse produced a positive reaction, such as rapid paw withdrawal

or sudden hindpaw licking, and the withdrawal time was recorded. The test was repeated 3 times with an interval of 10 min. The test was performed at 3, 7, 14, 21, 28, 35, 42, 49, 56, 63, 70, and 71 days postinjury.

Neuroelectrophysiology

The MEPs of the hindlimb were evaluated by electromyography as described in our previous research,[24] In brief, after intraperitoneal anesthesia, stimulating electrodes were placed on the surface of the skull corresponding to the cortical motor area. Then, the recording electrodes were inserted into the tibialis anterior muscle of the contralateral hindlimb. The reference electrode was subcutaneously inserted into tissue between the stimulating and recording electrodes. After the electrodes were fixed, the mean MEP values, including the latency and amplitude period, were recorded. The assay was performed before injury and at 56 and 57 days postinjury.

Western blot analysis

For protein extraction, RIPA buffer was used to lyse cells and tissue (10 mm of the spinal cord containing the injury epicenter). Protein concentrations were detected by using a Bicinchoninic acid (BCA) assay kit. The denatured proteins were electrophoretically transferred to a 10% SDS-PAGE gel and subsequently transferred to polyvinylidene fluoride (PVDF) membranes. The membranes were incubated at 4°C overnight with a mouse anti-acetylated tubulin monoclonal antibody (1:1,000; Proteintech, USA), rabbit anti-H3K27me3 antibody (1:1,000; CST, USA), rabbit anti-NeuroD1 antibody (1:1,000; Abcam, USA), rabbit anti-UTX antibody (1:1,000; Abcam, USA), actin (1:5,000; Abcam, USA), rabbit anti-β-tubulin antibody (1:1,000; CST, USA), and anti-GAPDH antibody (1:5,000; Abcam, USA). After the membranes were washed with 1% Tris-HCl+Tween (TBST) 3 times (15 min each), they were incubated with a horseradish peroxidase (HRP)-conjugated secondary antibody (1:5,000; Proteintech, USA) for 90 min. Immunoreactive bands were visualized using enhanced chemiluminescence.

qRT-PCR

Total RNA was isolated using TRIzol (Invitrogen, Waltham, MA, USA) and reverse transcribed using a PrimeScript kit (TaKaRa Bio, Otsu, Japan) according to the manufacturer's instructions. qRT-PCR was performed with SYBR qPCR master mix (TaKaRa Bio) and a ViiATM7 RT-PCR system (Applied Biosystems, Carlsbad, CA, USA). Glyceraldehyde-3-phosphate dehydrogenase (GAPDH) was used to normalize the results. The miR-24 primers were designed and provided by Sangon Biotech (Shanghai, China), and miR-U6 was used as an internal control. The 2-ΔΔCt method was applied to analyze the expression of the target genes. The primer sequences are shown in Tables S1.

Immunofluorescence

Cell immunofluorescence

After being washed with PBS three times (5 min each), cells were fixed with 4% paraformaldehyde for 15 min. After fixation, the cells were permeabilized with 0.5% PBST (Triton X-100 dissolved in PBS) at room temperature for 20 min and blocked with 4% BSA (dissolved in pure water) for 45 min. The cells were incubated with the following primary antibodies: a mouse anti-acetylated tubulin monoclonal antibody (1:200; Proteintech, USA), rabbit anti-tyrosinated tubulin polyclonal antibody (1:400; Millipore, USA), and rabbit anti-beta-III tubulin polyclonal antibody (1:400; Abcam, USA). The following day, secondary antibodies (anti-mouse immunoglobulin [IgG] antibodies or anti-rabbit IgG antibodies) were added for 1 h at 37°C.

Frozen section immunofluorescence

A 10-mm spinal cord segment containing the lesion epicenter was harvested and dehydrated for sectioning. Frozen sections were rewarmed for 15 min at room temperature and washed for 15 min with PBS as described above. Permeabilization and blocking were carried out as described above. The sections were incubated overnight with a rabbit anti-beta-III tubulin polyclonal antibody (1:400; Abcam, USA), rabbit anti-alpha acetylated tubulin polyclonal antibody (1:500; Cell Signaling Technology, USA), mouse anti-NeuN monoclonal antibody (1:500; Abcam, USA), rabbit anti-UTX antibody (1:200; Millipore, USA), and goat anti-5-HT antibody (1:400; ImmunoStar, USA). The next day, the sections were incubated with secondary antibodies (anti-mouse IgG antibodies, anti-rabbit IgG antibodies, or anti-goat IgG antibodies) for 1 h at room temperature. To visualize BDA^+ axons, the sections were incubated with Cy3-conjugated streptavidin (1:800; Jackson ImmunoResearch, USA) for 1 h at room temperature.

In situ hybridization

In situ hybridization was performed using a biotin-labeled miR-24-specific probe (Sangon Biotech, Shanghai, China) as previously described. The samples were fixed with 4% paraformaldehyde (prepared with diethyl pyrocarbonate [DEPC] water) for 12 h and then embedded in paraffin. After the sections (8 μm) were dewaxed with xylene, they were digested with proteinase K (20 μg/mL) at 37°C for 30 min. The sections were washed three times with PBS (prepared with DEPC) for 5 min each and then treated with prehybridization buffer for 1 h at room temperature. The prehybridization buffer was decanted, and the miR-24-specific probe was added overnight at 60°C. Then, the sections were washed with 2× saline sodium citrate (SSC) at 37°C for 10 min, washed twice with 1× SSC at 37°C for 5 min, and washed with 0.5× SSC at room temperature for 10 min, after which they were incubated with blocking solution (5% BSA in 0.1% PBST) for 1 h at 37°C. The blocking solution was removed, and Cy3-conjugated streptavidin (1:800, Jackson ImmunoResearch, USA) was added at 37°C for 50 min. To determine the localization of miR-24 in neurons, the sections were incubated with a primary antibody (anti-NeuN, 1:400; Abcam) at 4°C overnight and then incubated with the corresponding secondary antibodies (1:500; Abcam) for 1 h at room temperature.

ChIP sequencing (ChIP-seq)

The ChIP experiment and high throughput sequencing and data analysis were conducted by Seqhealth Technology (Wuhan, China). In brief, the cells were fixed in 4% formaldehyde for 10 min at room temperature and crosslinked with 0.125 M glycine for 5 min. Then, the

cells were lysed, and the nuclei were collected by centrifugation at 2,000 × *g* for 5 min. After treating with nucleus lysis buffer, the genome DNA was interrupted to 200–1,000 bp by sonication. Subsequently, 10% of the sonication-treated chromatin was termed "input," 80% was used for immunoprecipitation with the anti-UTX antibody (ChIP level, Abcam, USA) and termed "IP," and the remaining 10% was incubated with rabbit IgG as a negative control and termed "IgG." VAHTS universal DNA library prep kit for Illumina V3 (catalog no. ND607, Vazyme) was used to prepare high-throughput DNA sequencing libraries. The final sequencing process was performed by a Novaseq 6000 sequencer (Illumina, USA) with the PE150 model.

ChIP-qPCR

We applied ChIP-qPCR to determine whether UTX can bind to the promoter of miR-24. In brief, after cross-linking with formaldehyde and termination with glycine, lysis buffer containing protease inhibitor was added to the cells. Adherent cells were scraped off, pipetted, and transferred to 1.5-mL Eppendorf tubes. Western blotting was performed to detect the protein expression of UTX. We obtained the motif of miR-24, which combined UTX and constructed corresponding primers (Table S2). The remaining DNA fragments of "IP" above were collected for detecting expression of miR-24 by PCR.

Dual-luciferase reporter assay

A dual-luciferase reporter plasmid was constructed by RiboBio (Guangzhou, China). In brief, the 3′ UTR sequence of NeuroD1 was designed and amplified by PCR and was inserted into the pmiR-RB reporter vector to construct a plasmid. The mutated 3′ UTR of NeuroD1 was used as a control vector. These plasmids were cotransfected into a human renal epithelial cell line (293T cells) with agomir-24 or a control mimic. Subsequently, an equal volume of Dual-Glo luciferase reagent was added to the cells, and the fluorescence intensity of each group was detected by a microplate reader.

Statistical analysis

The data were analyzed with GraphPad Prism 7. All results are presented as the means ± standard deviations (SDs). Significant differences between two groups were analyzed by two-tailed unpaired Student's t test. We conducted ANOVA followed by Tukey's post hoc tests to analyze differences among multiple groups. Repeated-measures ANOVA was used to analyze the BMS scores at different time points. Statistical significance was set at a p value <0.05.

SUPPLEMENTAL INFORMATION

Supplemental Information can be found online at https://doi.org/10.1016/j.omtm.2020.12.004.

ACKNOWLEDGMENTS

This work was supported by the National Natural Science Foundation of China (grants 81874004, 81672174 and 81902224), the Science and Technology Commission of Hunan Province of China (grant 2017SK2061), and the Fundamental Research Funds for the Central Universities of Central South University (2020zzts270).

AUTHOR CONTRIBUTIONS

J.H., Y.C., and H.L. designed and supervised the study. Z.G., C.L., T.Q., and Y.X. did the experiment. Y.C., L.J., M.L., and Z.L. analyzed data. Z.G., C.L., and Y.C. wrote and revised the manuscript. All authors contributed to the manuscript.

DECLARATION OF INTERESTS

The authors declare no competing interests.

REFERENCES

1. Fouad, K., Krajacic, A., and Tetzlaff, W. (2011). Spinal cord injury and plasticity: opportunities and challenges. Brain Res. Bull. *84*, 337–342.
2. Fitzharris, M., Cripps, R.A., and Lee, B.B. (2014). Estimating the global incidence of traumatic spinal cord injury. Spinal Cord *52*, 117–122.
3. Jazayeri, S.B., Beygi, S., Shokraneh, F., Hagen, E.M., and Rahimi-Movaghar, V. (2015). Incidence of traumatic spinal cord injury worldwide: a systematic review. Eur. Spine J. *24*, 905–918.
4. Journal of Spinal Cord Medicine (2016). Spinal Cord Injury (SCI) 2016 Facts and Figures at a Glance. J. Spinal Cord Med. *39*, 493–494.
5. Rowland, J.W., Hawryluk, G.W., Kwon, B., and Fehlings, M.G. (2008). Current status of acute spinal cord injury pathophysiology and emerging therapies: promise on the horizon. Neurosurg. Focus *25*, E2.
6. Singh, A., Tetreault, L., Kalsi-Ryan, S., Nouri, A., and Fehlings, M.G. (2014). Global prevalence and incidence of traumatic spinal cord injury. Clin. Epidemiol. *6*, 309–331.
7. Khorasanizadeh, M., Yousefifard, M., Eskian, M., Lu, Y., Chalangari, M., Harrop, J.S., Jazayeri, S.B., Seyedpour, S., Khodaei, B., Hosseini, M., and Rahimi-Movaghar, V. (2019). Neurological recovery following traumatic spinal cord injury: a systematic review and meta-analysis. J. Neurosurg. Spine *30*, 1–17.
8. Silva, N.A., Sousa, N., Reis, R.L., and Salgado, A.J. (2014). From basics to clinical: a comprehensive review on spinal cord injury. Prog. Neurobiol. *114*, 25–57.
9. Hu, J., Lang, Y., Cao, Y., Zhang, T., and Lu, H. (2015). The Neuroprotective Effect of Tetramethylpyrazine Against Contusive Spinal Cord Injury by Activating PGC-1α in Rats. Neurochem. Res. *40*, 1393–1401.
10. Tran, A.P., Warren, P.M., and Silver, J. (2018). The Biology of Regeneration Failure and Success After Spinal Cord Injury. Physiol. Rev. *98*, 881–917.
11. Fawcett, J.W., and Verhaagen, J. (2018). Intrinsic Determinants of Axon Regeneration. Dev. Neurobiol. *78*, 890–897.
12. Trakhtenberg, E.F., and Goldberg, J.L. (2012). Epigenetic regulation of axon and dendrite growth. Front. Mol. Neurosci. *5*, 24.
13. Shin, J.E., and Cho, Y. (2017). Epigenetic Regulation of Axon Regeneration after Neural Injury. Mol. Cells *40*, 10–16.
14. Wahane, S., Halawani, D., Zhou, X., and Zou, H. (2019). Epigenetic Regulation Of Axon Regeneration and Glial Activation in Injury Responses. Front. Genet. *10*, 640.
15. Qureshi, I.A., and Mehler, M.F. (2015). Epigenetics and therapeutic targets mediating neuroprotection. Brain Res. *1628* (Pt B), 265–272.
16. Barker, S.J., and Tsai, L.H. (2017). MethyLock: DNA Demethylation Is the Epigenetic Key to Axon Regeneration. Neuron *94*, 221–223.
17. Cho, Y., and Cavalli, V. (2012). HDAC5 is a novel injury-regulated tubulin deacetylase controlling axon regeneration. EMBO J. *31*, 3063–3078.
18. Jaenisch, R., and Bird, A. (2003). Epigenetic regulation of gene expression: how the genome integrates intrinsic and environmental signals. Nat. Genet. *33* (*Suppl*), 245–254.
19. Hwang, J.Y., Aromolaran, K.A., and Zukin, R.S. (2017). The emerging field of epigenetics in neurodegeneration and neuroprotection. Nat. Rev. Neurosci. *18*, 347–361.
20. Agger, K., Cloos, P.A., Christensen, J., Pasini, D., Rose, S., Rappsilber, J., Issaeva, I., Canaani, E., Salcini, A.E., and Helin, K. (2007). UTX and JMJD3 are histone H3K27 demethylases involved in HOX gene regulation and development. Nature *449*, 731–734.

21. Lei, X., and Jiao, J. (2018). UTX Affects Neural Stem Cell Proliferation and Differentiation through PTEN Signaling. Stem Cell Reports *10*, 1193–1207.

22. Xu, J., Deng, X., Watkins, R., and Disteche, C.M. (2008). Sex-specific differences in expression of histone demethylases Utx and Uty in mouse brain and neurons. J. Neurosci. *28*, 4521–4527.

23. Tang, G.B., Zeng, Y.Q., Liu, P.P., Mi, T.W., Zhang, S.F., Dai, S.K., Tang, Q.Y., Yang, L., Xu, Y.J., Yan, H.L., et al. (2017). The Histone H3K27 Demethylase UTX Regulates Synaptic Plasticity and Cognitive Behaviors in Mice. Front. Mol. Neurosci. *10*, 267.

24. Ni, S., Luo, Z., Jiang, L., Guo, Z., Li, P., Xu, X., Cao, Y., Duan, C., Wu, T., Li, C., et al. (2019). UTX/KDM6A Deletion Promotes Recovery of Spinal Cord Injury by Epigenetically Regulating Vascular Regeneration. Mol. Ther. *27*, 2134–2146.

25. Mattick, J.S., and Makunin, I.V. (2006). Non-coding RNA. Hum. Mol. Genet. *15*, R17–R29.

26. Hu, J., Ni, S., Cao, Y., Zhang, T., Wu, T., Yin, X., Lang, Y., and Lu, H. (2016). The Angiogenic Effect of microRNA-21 Targeting TIMP3 through the Regulation of MMP2 and MMP9. PLoS ONE *11*, e0149537.

27. Li, F., and Zhou, M.W. (2019). MicroRNAs in contusion spinal cord injury: pathophysiology and clinical utility. Acta Neurol. Belg. *119*, 21–27.

28. Zhang, T., Ni, S., Luo, Z., Lang, Y., Hu, J., and Lu, H. (2019). The protective effect of microRNA-21 in neurons after spinal cord injury. Spinal Cord *57*, 141–149.

29. Hu, J.Z., Huang, J.H., Zeng, L., Wang, G., Cao, M., and Lu, H.B. (2013). Anti-apoptotic effect of microRNA-21 after contusion spinal cord injury in rats. J. Neurotrauma *30*, 1349–1360.

30. Jahan, I., Kersigo, J., Pan, N., and Fritzsch, B. (2010). Neurod1 regulates survival and formation of connections in mouse ear and brain. Cell Tissue Res. *341*, 95–110.

31. Lai, M., Pan, M., Ge, L., Liu, J., Deng, J., Wang, X., Li, L., Wen, J., Tan, D., Zhang, H., et al. (2020). NeuroD1 overexpression in spinal neurons accelerates axonal regeneration after sciatic nerve injury. Exp. Neurol. *327*, 113215.

32. Mironets, E., Wu, D., and Tom, V.J. (2016). Manipulating extrinsic and intrinsic obstacles to axonal regeneration after spinal cord injury. Neural Regen. Res. *11*, 224–225.

33. Venkatesh, I., Mehra, V., Wang, Z., Califf, B., and Blackmore, M.G. (2018). Developmental Chromatin Restriction of Pro-Growth Gene Networks Acts as an Epigenetic Barrier to Axon Regeneration in Cortical Neurons. Dev. Neurobiol. *78*, 960–977.

34. Van der Meulen, J., Speleman, F., and Van Vlierberghe, P. (2014). The H3K27me3 demethylase UTX in normal development and disease. Epigenetics *9*, 658–668.

35. Roidl, D., and Hacker, C. (2014). Histone methylation during neural development. Cell Tissue Res. *356*, 539–552.

36. Puttagunta, R., Tedeschi, A., Sória, M.G., Hervera, A., Lindner, R., Rathore, K.I., Gaub, P., Joshi, Y., Nguyen, T., Schmandke, A., et al. (2014). PCAF-dependent epigenetic changes promote axonal regeneration in the central nervous system. Nat. Commun. *5*, 3527.

37. Ma, T.C., and Willis, D.E. (2015). What makes a RAG regeneration associated? Front. Mol. Neurosci. *8*, 43.

38. Pataskar, A., Jung, J., Smialowski, P., Noack, F., Calegari, F., Straub, T., and Tiwari, V.K. (2016). NeuroD1 reprograms chromatin and transcription factor landscapes to induce the neuronal program. EMBO J. *35*, 24–45.

39. Westermann, S., and Weber, K. (2003). Post-translational modifications regulate microtubule function. Nat. Rev. Mol. Cell Biol. *4*, 938–947.

40. He, M., Ding, Y., Chu, C., Tang, J., Xiao, Q., and Luo, Z.G. (2016). Autophagy induction stabilizes microtubules and promotes axon regeneration after spinal cord injury. Proc. Natl. Acad. Sci. USA *113*, 11324–11329.

41. Kelliher, M.T., Saunders, H.A., and Wildonger, J. (2019). Microtubule control of functional architecture in neurons. Curr. Opin. Neurobiol. *57*, 39–45.

42. Cho, Y., Sloutsky, R., Naegle, K.M., and Cavalli, V. (2013). Injury-induced HDAC5 nuclear export is essential for axon regeneration. Cell *155*, 894–908.

43. Ertürk, A., Hellal, F., Enes, J., and Bradke, F. (2007). Disorganized microtubules underlie the formation of retraction bulbs and the failure of axonal regeneration. J. Neurosci. *27*, 9169–9180.

44. Hellal, F., Hurtado, A., Ruschel, J., Flynn, K.C., Laskowski, C.J., Umlauf, M., Kapitein, L.C., Strikis, D., Lemmon, V., Bixby, J., et al. (2011). Microtubule stabilization reduces scarring and causes axon regeneration after spinal cord injury. Science *331*, 928–931.

45. Ruschel, J., Hellal, F., Flynn, K.C., Dupraz, S., Elliott, D.A., Tedeschi, A., Bates, M., Sliwinski, C., Brook, G., Dobrindt, K., et al. (2015). Axonal regeneration. Systemic administration of epothilone B promotes axon regeneration after spinal cord injury. Science *348*, 347–352.

46. Lee, J.K., Geoffroy, C.G., Chan, A.F., Tolentino, K.E., Crawford, M.J., Leal, M.A., Kang, B., and Zheng, B. (2010). Assessing spinal axon regeneration and sprouting in Nogo-, MAG-, and OMgp-deficient mice. Neuron *66*, 663–670.

47. Basso, D.M., Fisher, L.C., Anderson, A.J., Jakeman, L.B., McTigue, D.M., and Popovich, P.G. (2006). Basso Mouse Scale for locomotion detects differences in recovery after spinal cord injury in five common mouse strains. J. Neurotrauma *23*, 635–659.

48. Chaplan, S.R., Bach, F.W., Pogrel, J.W., Chung, J.M., and Yaksh, T.L. (1994). Quantitative assessment of tactile allodynia in the rat paw. J. Neurosci. Methods *53*, 55–63.

49. Russell, F.A., Fernandes, E.S., Courade, J.P., Keeble, J.E., and Brain, S.D. (2009). Tumour necrosis factor alpha mediates transient receptor potential vanilloid 1-dependent bilateral thermal hyperalgesia with distinct peripheral roles of interleukin-1beta, protein kinase C and cyclooxygenase-2 signalling. Pain *142*, 264–274.